Flow Characteristics in Hot Pool of Sodium-Cooled Fast Reactor

Jung Yoon [a*], Seong-O Kim [a], Tae-Ho Lee [a]
[a]*Korea Atomic Energy Research Institute, Fast Reactor development Div., 1045 Daedeok-daero, Daejeon*
[*]*Corresponding author: jyoon@kaeri.re.kr*

1. Introduction

KAERI has developed the conceptual design of a pool-type Sodium-cooled Fast Reactor (SFR) with 600MWe capacity, and is currently establishing the design concept for a prototype SFR with 150MWe. From a fluid system design view point, the reactor hot pool thermal-hydraulics is related to various design issues such as decay heat removal operation, thermal stratification, measurements and so on. In the pool type reactor, all major components of Primary Heat Transport System (PHTS) are located inside the reactor vessel, and the flow characteristic in the hot pool region is quite complex. Thus, knowledge on multi-dimensional flow characteristics is essential for the system and component designs.

In this paper, a numerical analysis was performed to confirm the flow characteristics in the hot pool region of a pool-type SFR with a 600MWe capacity for various boundary conditions.

2. Methods and Results

2.1 Geometry and Condition

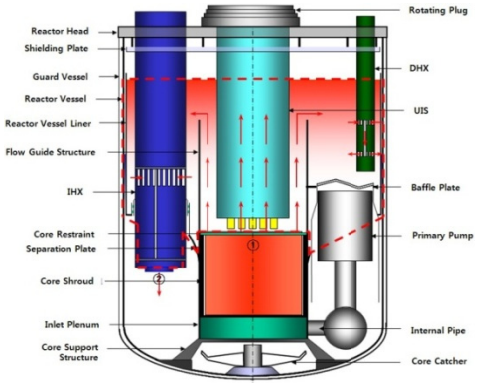

Fig. 1. Flow Path inside Reactor Vessel

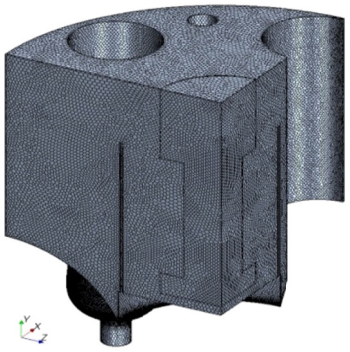

Fig. 2. Geometry of Hot Pool for CFD Analysis

The schematics and flow path inside the reactor vessel are shown in Fig. 1. The red arrows show the flow path of sodium. A hot pool consists of several components such as IHX, DHX and UIS. The calculation region for a CFD analysis is represented by the red dashed line. The geometry and mesh of the hot pool are shown in Fig. 2. Five cases are performed with a variation in the inlet flow rate and cooling capacity of a DHX. The boundary conditions in each case are shown in Table 1.

Table 1. Boundary Condition

Case	Inlet		DHX Cooling Capacity
	Temp.	Flow Rate	
Case1	510 °C	4,183kg/s	1.18MW
Case2			5.0MW
Case3			9.0MW
Case4		420kg/s	5.0MW
Case5			9.0MW

2.2 Methodology

A numerical analysis was performed by STAR-CCM+ V7.04.006[1]. A three-dimensional, 1/4 axisymmetric, steady-state flow are assumed. Conjugate heat transfer is considered between the sodium and SUS316, which is the material of the IHX and DHX. Also, material properties such as density, viscosity, conductivity and specific heat are functions of temperature[2]. The continuity, momentum, energy equation and SST k-w model are shown in Eq. (1) ~ (5).

IHX, DHX and UIS are treated as a porous media, and are considered for a pressure drop between the start and end point[3] as its inner flow patterns are not important in these analyses.

$$\frac{\partial}{\partial x_i}(\rho u_i) = 0 \tag{1}$$

$$\frac{\partial}{\partial x_i}(\rho u_i u_j) = -\frac{\partial p}{\partial x_i} + \frac{\partial}{\partial x_j}\left[\mu\left(\frac{\partial u_i}{\partial x_j} + \frac{\partial u_j}{\partial x_i} - \frac{2}{3}\delta_{ij}\frac{\partial u_i}{\partial x_j}\right)\right] + \frac{\partial}{\partial x_j}\left(-\rho\overline{u_i' u_j'}\right) \tag{2}$$

$$\nabla\cdot\left(\vec{v}(\rho E + p)\right) = \nabla\cdot\left(k_{eff}\nabla T - \sum_j h_j\vec{J_j} + \left(\overline{\overline{\tau_{eff}}}\cdot\vec{v}\right)\right) + S_h \tag{3}$$

$$\frac{\partial}{\partial x_i}(\rho u_i k) = \frac{\partial}{\partial x_j}\left(\Gamma_k\frac{\partial k}{\partial x_j}\right) + G_k - Y_k + S_k \tag{4}$$

$$\frac{\partial}{\partial x_i}(\rho u_i \omega) = \frac{\partial}{\partial x_j}\left(\Gamma_\omega \frac{\partial k}{\partial x_j}\right) + G_\omega - Y_\omega + S_\omega \qquad (5)$$

2.3 Result

The velocity and temperature distributions in a DHX section are shown in Fig. 3 and 4. The mass flow rate of upper the 3 cases (Case1, 2, 3) is 4,183kg/s and lower 2 cases (Case4, 5) is 420kg/s. In the case of 4,183kg/s, a large vortex is created, and mixing effect of pool inside is maximized according to a change in the cooling capacity of DHX. For 420kg/s, a vertical downward flow below DHX is created and mixing effect is minimized. Nevertheless, the velocity around the DHX of low mass flow rate cases is larger than other places in the plane section because the cooling capacity of the DHX affects around a flow pattern of the DHX.

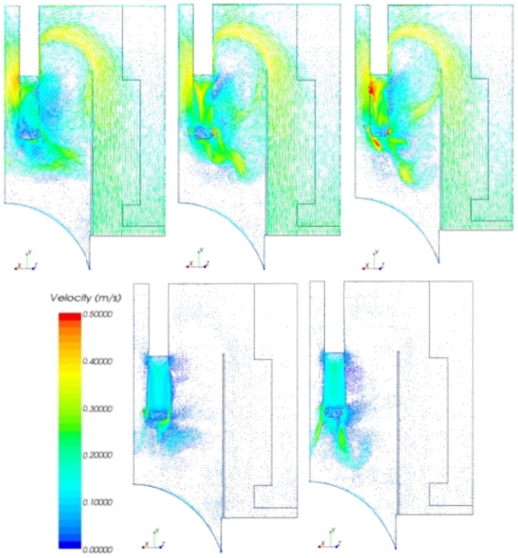

Fig. 3. Velocity Vector in DHX Section

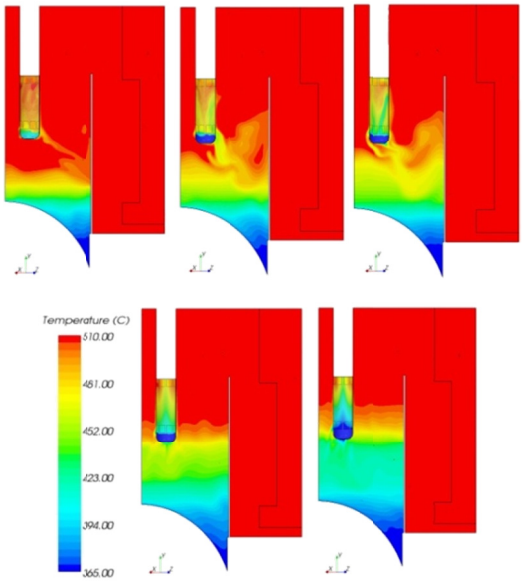

Fig. 4. Temperature Distribution in DHX Section

The mass flow rate of the DHX inlet in each case is shown in Table 2. Although mass flow rate of core outlet in cases 4 and 5 is much smaller than cases 1, 2 and 3, the mass flow rates of the DHX inlet in cases 4 and 5 are not small in comparison with case 1, 2 and 3. According to the increase in cooling capacity of DHX, the flow inside the DHX becomes active and affects the flow around DHX.

The temperature difference between DHX inlet and outlet in each case is shown in Table 3. As the cooling capacity of the DHX is increased, the temperature difference of the DHX inlet and outlet is increased. Also the temperature differences of cases 4 and 5 are bigger than those of cases 1, 2 and 3. Since the flow of cases 4 and 5 is not mixed well, the cooling ability of the DHX is maximized. Therefore, the temperature difference of the DHX inlet and outlet depends on the cooling capacity of the DHX rather than the mass flow rate of core outlet.

Table 2. Mass Flow Rate of DHX

Case	Inlet Flow Rate	DHX Cooling	Flow Rate (No H.S.)	Flow Rate
Case1	4,183kg/s	1.18MW	13.06kg/s	38.67kg/s
Case2		5.0MW		63.51kg/s
Case3		9.0MW		78.46kg/s
Case4	420kg/s	5.0MW	7.54kg/s	35.99kg/s
Case5		9.0MW		42.75kg/s

Table 3. Temperature difference of DHX

Case	DHX Cooling	Temp.(°C)		
		IN	OUT	dT
Case 1	1.18MW	507.0	486.7	20.3
Case 2	5.0MW	505.9	457.1	48.9
Case 3	9.0MW	505.2	434.3	70.9
Case 4	5.0MW	508.8	425.9	82.9
Case 5	9.0MW	508.4	385.2	123.2

3. Conclusions

A numerical analysis in the hot pool of a SFR was performed using STAR-CCM+. The internal major components of a hot pool are modeled, and calculations are performed with variations of the inlet flow rate and cooling capacity of a DHX. The flow and temperature distributions were shown to be influenced by the cooling capacity of the DHX rather than the mass flow rate of the core outlet. The obtained flow characteristics and developed methodology will be utilized for an assessment of PHTS internal arrangement of a prototype SFR.

REFERENCES

[1] STAR-CCM+ 7.04.006 User Guide, CD-adapco, 2012.
[2] J.W. Han, Thermal Hydraulic Analysis of 600MWe Demonstration Sodium-cooled Fast Reactor, KAERI, 2011.
[3] I.E. Idelchik, Handbook of Hydraulic Resistance, 3rd Edition, Begell House, pp. 75-110, 2005.
[4] C.K. Park, Input Data of Safety Analysis in Conceptual Design of Demonstration Reactor, KAERI, 2010.